CARBON DIOXIDE AND CLIMATIC CHANGE

SYUKURO MANABE

Geophysical Fluid Dynamics Laboratory/NOAA
Princeton University
Princeton, New Jersey

1. INTRODUCTION

According to the observations at Mauna Loa and other stations, the atmospheric CO_2 concentration is about 335 ppm at present and is increasing continuously. In the latter half of the next century the CO_2 concentration may reach 600 ppm, which is twice as much as the preindustrial concentration of 290 ppm (Geophysics Study Committee, 1977).

It has been suggested that such an increase in CO_2 concentration may lead to the general warming of climate (see, for example, Callendar, 1938). At the Geophysical Fluid Dynamics Laboratory of the NOAA, the study of climate change resulting from the future increase of atmospheric CO_2 concentration has been the subject of a long-term research project during the past 15 years. This article reviews some of the results from this research project.

ADVANCES IN GEOPHYSICS, VOLUME 25

ISBN 0-12-018825-2

2. Historical Background

In the latter half of the nineteenth century, Tyndall (1863) and Arrhenius (1896) suggested that a climate change may be induced by a change of CO_2 concentration in the atmosphere. These works were followed by the studies of Callendar (1938), Plass (1956), Kondratiev and Niilisk (1960), Kaplan (1960), and Möller (1963). In these studies, the CO_2-induced warming was evaluated from a condition of radiative heat budget at the earth's surface. I shall discuss briefly these studies before discussing the results from mathematical models of climate.

Although the atmospheric CO_2 absorbs solar radiation at near-infrared wavelength, the magnitude of the absorbed energy is very small. On the other hand, it strongly absorbs and emits terrestrial radiation at the wavelength of ~12–18 μm. In his study, Callendar shows that additional CO_2 in the atmosphere increases the downward flux of terrestrial radiation. To satisfy the condition of the surface heat balance, this CO_2-induced change of radiative flux should be compensated by an increase in the upward terrestrial radiation resulting from an increased surface temperature, if other components of surface heat balance remain unchanged. From consideration of the surface heat balance described above, Callendar estimated the CO_2-induced rise of surface temperature.

Most of the studies mentioned above employ similar approaches for the estimation of the CO_2-induced warming of the earth's surface, although there are some differences among them. For example, Kaplan takes into consideration the effect of cloud cover on the CO_2-induced change in the downward flux of terrestrial radiation. Kondratiev and Niilisk incorporate in their computation the effect of overlapping between an absorption band of water vapor and that of CO_2.

Möller attempted to improve these estimates by taking into consideration the effect of CO_2-induced change of water vapor in the atmosphere. He noted that the climatological distribution of relative humidity in the troposphere changes little with season despite a large change of air temperature. For example, an increase in air temperature is accompanied by an increase in absolute humidity of air, keeping the relative humidity unchanged. Therefore, the CO_2-induced change in the temperature of the earth's surface is accompanied by not only a change of temperature but also a change of absolute humidity of the overlying air which, in turn, causes a change in the downward flux of terrestrial radiation at the earth's surface. The change in absolute humidity also affects the absorption of solar radiation and, accordingly, the amount of solar radiation reaching the earth's surface. Möller estimated the warming of the earth's surface resulting from these increases of both terrestrial and solar radiation. For this purpose, he employed the following assumption:

$$d[S(W(T_s)) - E(T_s, W(T_s), C)] = 0 \tag{2.1}$$

where S is the net downward solar radiation; E is the net upward terrestrial radiation at the earth's surface; W is the total liquid equivalent of water vapor; C is the CO_2 concentration of air; T_s is the temperature of the earth's surface. E is a function of only T_s and W because the vertical distributions of relative humidity and static stability are assumed to be preserved despite the CO_2-induced temperature change. Carrying out the differentiation on the left-hand side of Eq. (2.1), one gets

$$\frac{\partial S}{\partial W}\frac{\partial W}{\partial T_s}dT_s - \frac{\partial E}{\partial T_s}dT_s - \frac{\partial E}{\partial W}\frac{dW}{dT_s}dT_s - \frac{\partial E}{\partial C}dC = 0 \tag{2.2}$$

From this equation, one can obtain the following relation which gives the temperature change dT_s resulting from the change in CO_2 concentration dC:

$$dT_s = \frac{\partial E/\partial C}{(\partial S/\partial W)(dW/dT_s) - \partial E/\partial T_s - (\partial E/\partial W)(dW/dT_s)}dC \tag{2.3}$$

From this formula, Möller obtained rather surprising results: an increase in the water vapor content of the atmosphere with rising temperature causes a self-amplification effect which results in a large temperature change. When the air temperature is around 15°C, the doubling of CO_2 content results in a large temperature increase of 10°C. For other temperatures, the results may be completely different. Möller obtained such a wide variety of results because the denominator on the right-hand side of Eq. (2.3) is small and changes in sign and magnitude, depending upon the surface temperature T_s. In other words, the net upward radiation at the earth's surface hardly increases with increasing surface temperature because of the dependence of absolute humidity upon the atmospheric temperature. On the other hand, the net upward radiation increases significantly with increasing surface temperature when it is assumed that the absolute humidity of air is unchanged by an increase of atmospheric CO_2 concentration. Therefore, the earlier studies of Callendar and others yielded less arbitrary results.

The study of Möller described above exposed the basic difficulty of the surface radiation balance approach, which does not take into consideration the CO_2-induced changes in other components of the surface heat balance. It is expected that the change in the atmospheric CO_2 concentration alters not only the net radiative flux, but also the boundary-layer exchanges of sensible and latent heat between the earth's surface and the atmosphere. Accordingly, the following balance requirement [instead of Eq. (2.1)] should hold at the earth's surface:

$$d(S - E - H) = 0 \tag{2.4}$$

where H is the sum of sensible and latent heat fluxes from the earth's surface into the atmosphere. In order to evaluate the change in H, it is necessary to consider not only the heat balance of the earth's surface, but also that of the atmosphere. Instead, Möller assumed that $dH = 0$. This is why his approach produced a result which is extremely sensitive to the surface temperature.

Recently, Newell and Dopplick (1979) attempted to estimate the CO_2-induced warming of the earth's surface by employing a surface energy balance method which incorporates not only the CO_2-induced change of radiative flux E but also that of H. Neglecting the CO_2-induced change in atmospheric water vapor W and solar flux S, one gets the following relationship from Eq. (2.4):

$$dT_s = -\frac{\partial E/\partial C}{\partial E/\partial T_s + \partial H/\partial T_s}\, dC \tag{2.5}$$

In order to estimate the CO_2-induced warming from Eq. (2.5), it is necessary to compute $\partial H/\partial T_s$. For this purpose, they made an unrealistic assumption that the change of surface temperature is not accompanied by the changes of temperature and absolute humidity of the overlying air. This assumption is responsible for the strong dependence of H upon surface temperature, i.e., the large value of $\partial H/\partial T_s$. (Note that it was assumed that the boundary-layer fluxes of sensible and latent heat are proportional to the air–surface difference of temperature and absolute humidity, respectively.) Thus, they obtained a very small value of $\partial T_s/\partial C$ from Eq. (2.5). In short, surface temperature can hardly change in response to a CO_2 increase when it is assumed that the temperature and absolute humidity of the overlying air do not change.

To evaluate H and its dependence on other variables, it is obviously necessary to consider not only the heat balance of the earth's surface but also that of the atmosphere. In the following section, the CO_2-induced change of the atmospheric temperature is discussed based upon the results from radiative, convective models of the atmospheric–surface system.

3. Radiative, Convective Equilibrium

In order to evaluate the CO_2-induced change of atmospheric temperature, Manabe and Wetherald (1967) used a "radiative, convective model of the atmosphere." This one-dimensional model consists of a system of the equations which represent the effects of radiative transfer and vertical convective mixing upon the heat balance of the atmosphere. As discussed

below, the model may be used for the determination of the vertical distribution of the global mean temperature of the atmosphere in thermal equilibrium. By comparing the two thermal equilibria for the normal and above-normal concentrations of atmospheric CO_2, Manabe and Wetherald estimated the change of the global mean atmospheric temperature which occurs in response to an increase in the CO_2 concentration of air. It turned out that their study was useful for getting a preliminary insight into the physical mechanisms responsible for the CO_2-induced temperature change in the atmosphere. This section begins with the definition of radiative, convective equilibrium followed by a discussion of the CO_2-induced change of the atmospheric temperature.

3.1. Approach toward a Thermal Equilibrium

An atmosphere in radiative, convective equilibrium satisfies the following conditions:

(1) The net radiative flux at the top of the atmosphere is zero.
(2) The lapse rate of the atmosphere does not exceed a certain critical lapse rate because of the stabilizing effect of convection and other dynamical processes.
(3) In a layer where the lapse rate is subcritical (convectively stable), the condition of local radiative equilibrium is satisfied, i.e., the net radiative flux is zero.
(4) The heat capacity of the earth's surface is zero. This implies that, at the earth's surface, the net downward flux of radiation is equal to the upward convective heat flux.

In order to determine the temperature distribution of the atmosphere in radiative, convective equilibrium, Manabe and Wetherald employed "the time integration method" in which the state of radiative, convective equilibrium was approached asymptotically through the numerical time integration of the following equation:

$$C_p \frac{\partial T}{\partial t} = Q_R + Q_c \tag{3.1}$$

where C_p is the specific heat of air; T is temperature; Q_R and Q_c are heating rate per unit mass due to radiation and convection, respectively. For the computation of heating (or cooling) due to solar and terrestrial radiation, the effects of water vapor, carbon dioxide, ozone, and cloud cover were taken into consideration. The effect of convection was incorporated into the model by use of the very simple procedure of

"convective adjustment." This procedure involves the adjustment of the lapse rate to a critical value whenever it becomes supercritical during the course of a time integration. The adjustment was made such that the sum of internal and potential energy was unaltered. For their study, the critical lapse rate was chosen to be 6.5°C/km in reference to the static stability of the actual atmosphere. Based upon the assumption that the earth's surface has no heat capacity, the net downward radiative flux received by the earth's surface was immediately returned to the lowest layer of the atmosphere, inducing the convective adjustment in the overlying layer. Following the suggestion of Möller, it was also assumed that the model atmosphere maintains a given distribution of relative humidity. As air temperature changed during the course of a time integration, the distribution of absolute humidity was continuously updated such that relative humidity remains unchanged. On the other hand, it was assumed that the uniform mixing ratio of CO_2 and the vertical distributions of cloud cover and ozone did not change with time. In addition, the globally averaged, annual mean insolation was prescribed at the top of the model atmosphere throughout the course of a numerical time integration.

Figure 1 illustrates how the temperature of the model atmosphere approaches the equilibrium value starting from the initial condition of a cold

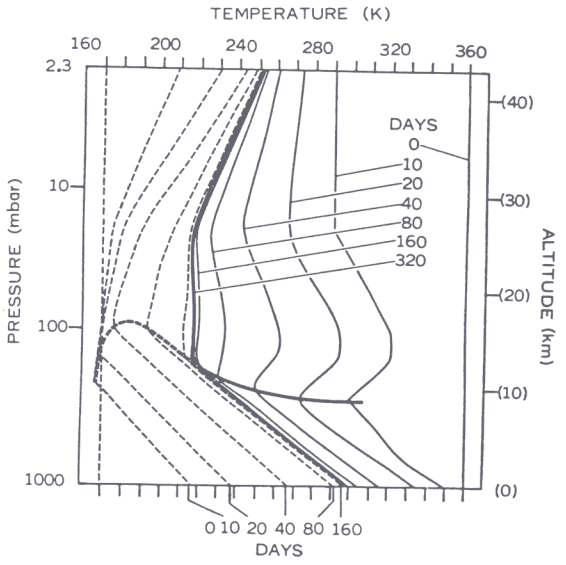

FIG. 1. Approaches toward the state of radiative, convective equilibrium. The solid and dashed lines show the approaches from warm and cold isothermal atmospheres, respectively. (From Manabe and Wetherald, 1967.)

(or warm) isothermal atmosphere. Toward the end of each time integration, the model atmosphere attains the realistic structure consisting of a convective troposphere and a stable stratosphere. The net incoming solar radiation becomes almost exactly equal to the outgoing terrestrial radiative at the top of the atmosphere, indicating that the atmosphere–surface system of the model is in radiative equilibrium as a whole. In the stable model stratosphere, the radiative heating (or cooling) is equal to zero, satisfying the condition of local radiative equilibrium. On the other hand, the model troposphere is not in radiative equilibrium. The total radiative heat loss from the model troposphere is equal to the net radiative heat gain by the earth's surface, implying the convective transfer of heat from the earth's surface to the atmosphere of the model.

3.2. Equilibrium Response

To evaluate the sensitivity of the model atmosphere to changes in atmospheric CO_2 concentration, a set of numerical time integrations was performed with the radiative, convective model of the atmosphere described above. Figure 2 illustrates the vertical distributions of the equilibrium temperature of the model atmosphere with the normal, half the normal, and twice the normal concentration of CO_2. This figure indicates that, in response to the doubling of the atmospheric CO_2, the temperature of the model troposphere increases by about 2.3°C whereas that of the middle stratosphere decreases by several degrees. In addition, it reveals that the magnitude of the warming resulting from the doubling of CO_2 concentration is approximately equal to the magnitude of the cooling from the halving of CO_2 concentration. This result suggests that CO_2-induced temperature change is not linearly proportional to the change in CO_2 concentration. Instead, it is proportional to the change in the logarithm of CO_2 concentration (see also the results of Rasool and Schneider, 1971; Augustson and Ramanathan, 1977).

The physical process of the warming due to an increase in CO_2 concentration has traditionally been explained by citing the greenhouse effect as an analogy. However, this is not a satisfactory analogy for the warming of the model troposphere. The warming process may be understood by considering the CO_2-induced change in the emissivity of the model atmosphere. In response to an increase in CO_2 concentration, the infrared opacity of the model atmosphere increases, raising the altitude of the effective source of the infrared emission into the space. Since the tropospheric temperature decreases with increasing altitude, this results in the lowering of the effective emission temperature for the outgoing radiation

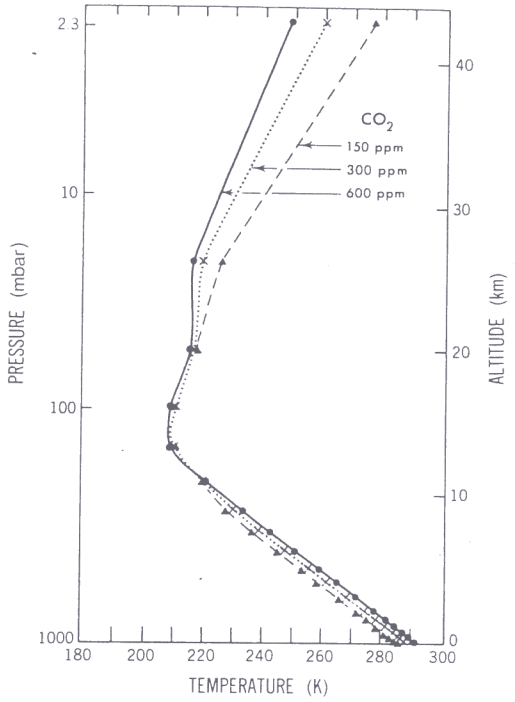

FIG. 2. Vertical distributions of temperature in radiative, convective equilibrium for various values of atmospheric CO_2 concentration, i.e., 150, 300, 600 ppm by volume. (From Manabe and Wetherald, 1967.)

and reduces the intensity of upward radiation at the top of the model atmosphere. In order to satisfy the condition that the outgoing terrestrial radiation be equal to the net incoming solar radiation at the top of the model atmosphere, it is therefore necessary to raise the temperature of the model troposphere, preventing the reduction of the outgoing terrestrial radiation.

In response to this warming, the absolute humidity of the model troposphere increases. This causes further increase in the infrared opacity of the atmosphere and raises the altitude of the effective source of the outgoing radiation. Thus, the temperature of the model troposphere must increase in order to maintain the radiation balance of the earth–atmosphere system. In addition, this increase of absolute humidity increases the fraction of solar radiation absorbed by the model troposphere and further enhances the CO_2-induced warming. Because of these positive feedback effects, the radiative, convective equilibrium of a model with a fixed

distribution of relative humidity is twice as sensitive to a doubling of the atmospheric CO_2 concentration as that of another model with a fixed distribution of absolute humidity (Manabe and Wetherald, 1967). In short, the change of absolute humidity resulting from the change in air temperature significantly enhances the sensitivity of climate.

The above discussion implies that the earth's surface and the troposphere of the model are strongly coupled. The CO_2-induced warming of the coupled system results from the reduction in the radiative cooling of the system. The CO_2-induced change in the turbulent heat flux from the earth's surface to the overlying troposphere is essentially determined by the change in radiative heat deficit of the troposphere, which is equal to the change in the net radiative heat energy absorbed by the earth's surface.

As pointed out already, the temperature of the model stratosphere reduces in response to an increase of the CO_2 concentration in the atmosphere. In order to comprehend this result, it is necessary to recognize that the radiative heat budget of the model stratosphere is essentially maintained as a balance between the heating due to the absorption of the solar ultraviolet radiation by ozone and the net radiative cooling due to carbon dioxide. The increase of the emissivity of air resulting from an increase in CO_2 concentration enhances this cooling due to CO_2 and is responsible for the reduction of the temperature in the model stratosphere.

It is significant that the CO_2-induced change in the temperature of the model atmosphere is proportional to the change in the logarithm of atmospheric CO_2 concentration rather than the concentration itself. This is because the emissivity of CO_2 is approximately proportional to the logarithm of the CO_2 concentration.

Table I tabulates the changes of surface temperature due to the doubling of the atmospheric CO_2 concentration. The data were obtained from

TABLE I. INCREASE OF SURFACE AIR TEMPERATURE OF THE ATMOSPHERE IN RADIATIVE, CONVECTIVE EQUILIBRIUM RESULTING FROM THE DOUBLING OF CO_2 CONCENTRATION OF AIR

Reference	ΔT (°C)
Manabe and Wetherald (1967)	2.3
Manabe (1971)	1.9
Ramanathan (1976)	1.5
Wang *et al.* (1976)	1.6[a]
Augustsson and Ramanathan (1977)	2.0

[a] The estimates of Wang *et al.* (1976) are inferred from the result of numerical experiments in which CO_2 concentration is increased by a factor of 1.25.

radiative, convective models of the atmosphere developed by various authors. The magnitudes of warming contained in this table range from 1.5° to 2.3°C and are not very different from one another.

One must keep in mind, however, that the radiative, convective models used to obtain the results in Table I do not include various feedback mechanisms which can alter the sensitivity of climate. For example, the study of Augustson and Ramanathan quoted in Table I demonstrates that the sensitivity of climate can change significantly when the assumption of fixed cloud cover is abandoned. A recent study of Hansen *et al.* (1981) with a radiative, convective model indicates that the sensitivity of a model climate depends significantly upon the choice of a parameterization of the moist convective process.

Obviously, it is necessary to use a more comprehensive model of climate for the further discussion of the CO_2–climate sensitivity problem. Nevertheless, there is little doubt that a radiative, convective model is a very useful tool for getting a preliminary insight into this problem and identifying various factors which affect the sensitivity of climate.

4. Distribution of the Global Climate Change

In the preceding section, the CO_2-induced change of global mean temperature is discussed based upon the results from one-dimensional models of the atmosphere in radiative, convective equilibrium. In order to discuss the latitudinal or geographical distribution of the CO_2-induced climate change, however, it is necessary to use a three-dimensional model of climate in which the effects of the atmospheric circulation and other physical process are explicitly taken into account. Furthermore, such a three-dimensional model is indispensable for the comprehensive assessment of the influences of various feedback mechanisms upon the sensitivity of climate.

Almost 25 years have passed since the pioneering attempts of Phillips (1956) and Smagorinsky (1963) to simulate the atmospheric general circulation by the use of three-dimensional, dynamical models of the atmosphere. Owing to the improvement of climate models and rapid advance of computer technology, it has become possible to simulate many of the large-scale characteristics of atmospheric circulation and climate by these models.

Encouraged by the similarity between the model climate and the actual climate, Manabe and Wetherald (1975) made the first attempt to study the CO_2-induced climate change by the use of a general circulation model of the atmosphere. For economy of computer time, their model had a limited

computational domain with an idealized geography and had no seasonal variation of insolation. Nevertheless, this study, together with a companion study by Manabe and Wetherald (1980), yielded a preliminary insight into how the latitudinal distribution of the CO_2-induced climate change may be determined. These studies were followed by the investigations of Manabe and Stouffer (1979, 1980) and Manabe *et al.* (1981) which employed a global model of the joint atmosphere–mixed-layer ocean system with seasonal variation of insolation. This section discusses the latest results from this global model. Some of the conclusions from the earlier studies mentioned above will be incorporated in this discussion.

4.1. General Circulation Model

A general circulation model of climate is a prognostic system of equations representing the physical and dynamical processes which control climate. As was done to obtain a radiative, convective equilibrium solution of the atmosphere, a statistically stationary climate is approached asymptotically through the long-term integration of the general circulation model.

The general circulation model of climate used by Manabe and Stouffer consists of three major components: (1) a general circulation model of the atmosphere, (2) a heat- and water-balance model of the continental surface, and (3) a static, mixed-layer model of the ocean. Figure 3 contains the box diagram illustrating the basic structure of the model. The structure of each component is briefly described below.

The general circulation model of the atmosphere predicts the changes of the vertical component of vorticity, horizontal divergence, tempera-

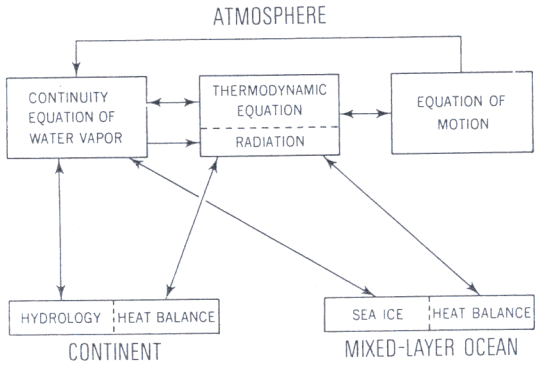

FIG. 3. Box diagram illustrating the basic structure of the atmosphere–mixed-layer ocean model of Manabe and Stouffer (1980).

ture, moisture, and surface pressure based upon the equation of motion, the thermodynamical equation, and the continuity equations of air mass and water vapor. The horizontal distributions of these predicted variables are represented by a finite number of spherical harmonics. The model has a global computational domain with realistic geography.

For the computation of solar and terrestrial radiation, the distributions of ozone and cloud cover are prescribed beforehand and the uniform concentration of carbon dioxide is set differently for each experiment, whereas the distribution of water vapor is determined from the prognostic system of water vapor.

Condensation of water vapor is predicted whenever supersaturation is indicated in the computation of the continuity equation of water vapor. Snowfall is predicted when air temperature near the earth's surface falls below the freezing temperature. Otherwise, rainfall is predicted.

The temperature of the continental surface is determined so that it satisfies the requirement of the heat balance. The changes of soil moisture and snow depths are obtained from the budget computations of water and snow, respectively.

The ocean model is a vertically isothermal and static water layer of uniform thickness with provision for a sea ice layer. The thickness of 68 m is chosen to ensure that the heat storage associated with the seasonal variation of observed sea surface temperature is correctly modeled. The rate of temperature change of the mixed-layer ocean is computed based upon the budget among surface heat fluxes. For this computation, the contributions of the horizontal heat transport by ocean currents and heat exchange between the mixed layer and the deeper layer of ocean are not taken into consideration. In the presence of sea ice, the temperature of the underlying water of the mixed-layer ocean is at the freezing point and the heat flux through the ice is balanced by the latent heat of freezing and melting at the bottom of the ice. This process, together with the melting at the upper surface of the ice, sublimation, and snowfall, determines the change of ice thickness. The albedo of sea ice and continental snow is assumed to vary between 50 and 80% depending on latitude and its thickness. Smaller values are assigned for thin sea ice, thin snow, or melting surface of sea ice.

4.2. Simulated Climate

In order to determine with confidence the CO_2-induced change of climate based upon the results from a numerical experiment with a mathematical model, it is necessary that the model be capable of reproducing the seasonal and geographical variation of climate. This section contains a

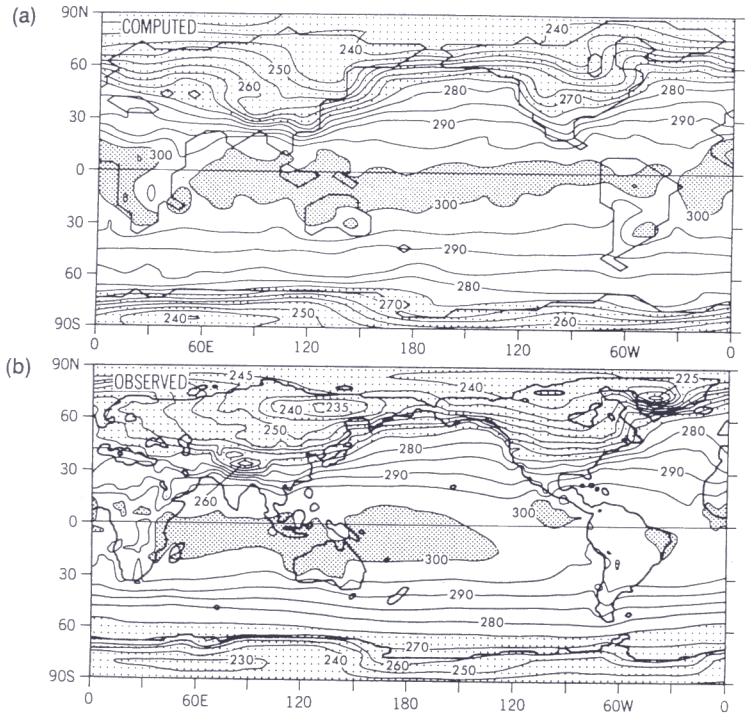

FIG. 4. Geographical distribution of monthly mean surface air temperature (kelvins) in February: (a) computed distribution from the 1 × CO_2 experiment (Manabe and Stouffer, 1980); (b) observed distribution (Crutcher and Meserve, 1970; Taljaad *et al.*, 1969).

brief description of climate as simulated by the Manabe–Stouffer model described in Section 4.1.

The model climate is obtained as a statistically stationary state emerging from a 15-yr integration of the model. The initial condition for this time integration is an isothermal and dry atmosphere at rest with an isothermal mixed-layer ocean. Accordingly, it is clear that the success or failure of the climate simulation does not depend critically upon the specific choice of the initial condition.

In Fig. 4, the geographical distribution of monthly mean surface air temperature in February obtained from the standard (1 × CO_2)[1] experiment is compared with the corresponding observed distribution from the data compiled by Crutcher and Meserve (1970) and Taljaad *et al.* (1969). On the basis of this comparison, one can identify unrealistic features in the model distribution. For example, the computed surface air tempera-

[1] n × CO_2 denotes n times the normal CO_2 concentration.

ture is too low over the North Atlantic Ocean due to the absence of the effect of poleward heat transport by ocean currents in the model ocean. On the other hand, it is too high in the Southern Hemisphere, particularly along the periphery of Antarctica, probably because the prescribed cloud amount in the Southern Hemisphere is too small as compared with the observed amount. Nevertheless, it is clear that the model successfully reproduces the large-scale characteristics in the global distribution of the observed surface air temperature.

Figure 5 illustrates the geographical distribution of the difference in surface air temperature between August and February. It is expected that the difference yields information on the approximate magnitude of the seasonal variation except in the equatorial region where semiannual variation predominates. This figure indicates that the model fails to simulate the belt of relatively large temperature variation around 30° S. It does,

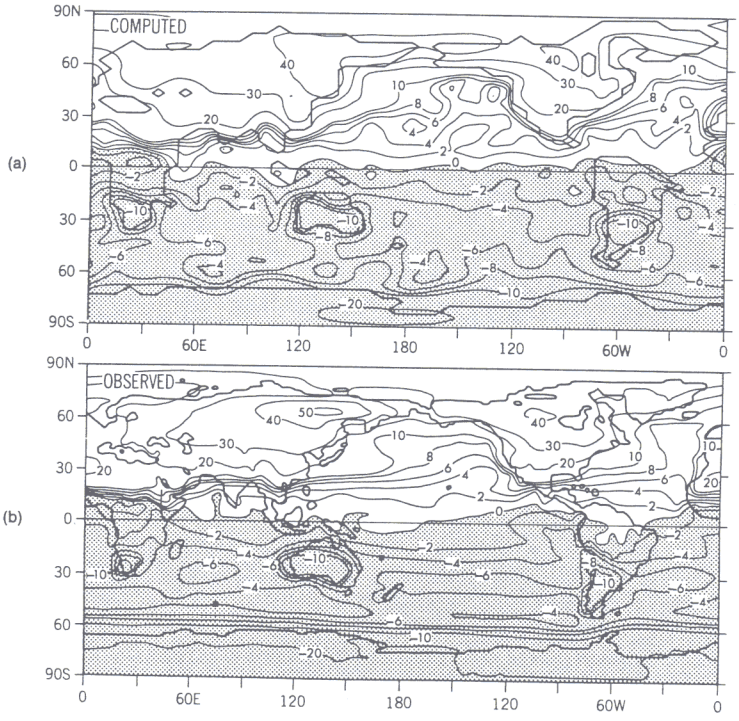

FIG. 5. Geographical distribution of surface air temperature difference (kelvins) between August and February: (a) computed distribution from the 1 × CO_2 experiment (Manabe and Stouffer, 1980); (b) observed distribution [from the data compiled by Crutcher and Meserve (1970) and Taljaad *et al.* (1969)]. Note that the contour interval is 2 K when the absolute value of the difference is less than 10 K and is 10 K when it is more than 10 K.

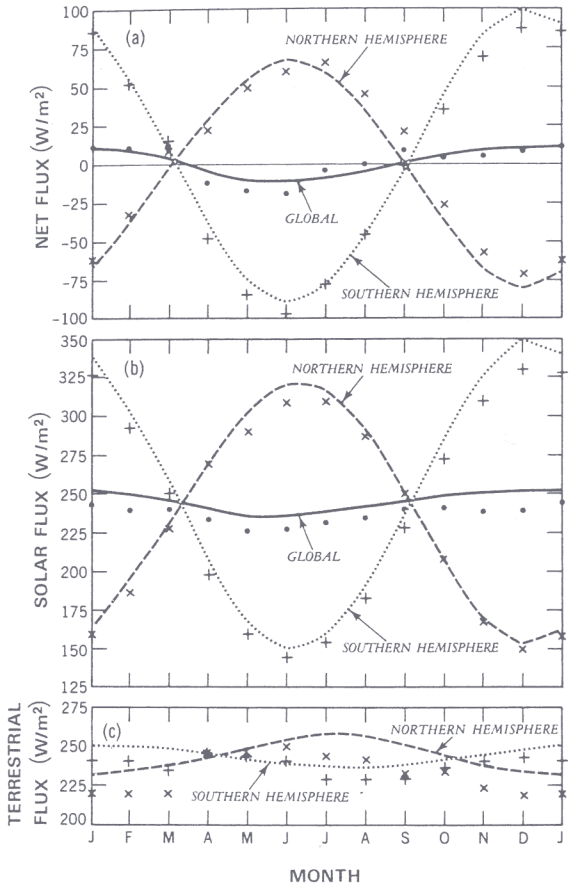

FIG. 6. Seasonal variation of hemisphere and global mean values of radiative fluxes at the top of the atmosphere (Manabe and Stouffer, 1980): (a) net radiative flux (i.e., net downward solar flux minus upward terrestrial flux); (b) net downward solar flux (i.e., incoming solar flux minus reflected flux); (c) upward terrestrial flux. Observed fluxes are deduced from satellite observation by Ellis and Vonder Haar (1976) in the Northern Hemisphere (×), Southern Hemisphere (+), and the entire globe (●).

however, reproduce the region of large annual temperature range over the northeastern part of the Eurasian continent and the northern part of North America. In general, the simulated distribution resembles the observed distribution quite well.

To evaluate the performance of the model in reproducing the overall radiation budget of the atmosphere–ocean system, Fig. 6 is constructed. This figure illustrates the seasonal variation of hemispheric and global

mean values of solar, terrestrial, and net radiative fluxes at the top of the model atmosphere. For comparison, the values of the radiative fluxes deduced from satellite observation by Ellis and Vonder Haar (1976) are added to the figure. This comparison reveals that the agreement between the computed and observed fluxes is good, although both the solar and terrestrial fluxes of the model are slightly larger than the observed fluxes. The agreement is particularly noteworthy if one recalls that the prescribed distribution of cloud cover in the model atmosphere has no seasonal variation. These results suggest that the variation of cloud cover has a relatively small role in determining the seasonal variation of hemispheric mean values of radiation fluxes and surface air temperature of the atmosphere. This encourages one to speculate that the cloud cover may not have a dominant effect in determining the sensitivity of global (or hemispheric) mean temperature.

4.3. Design of Sensitivity Experiment

The climatic effect of an increase in atmospheric CO_2 is investigated based upon the comparison between two climates with normal and four times the normal CO_2 concentration. One could have investigated the consequence of a smaller increase of the CO_2 concentration, which is more likely to occur in the future. Instead, the atmospheric CO_2 concentration is increased by a factor of four for the ease of discriminating the CO_2-induced change from the natural fluctuation of the model climate. Figure 7 illustrates how the global mean sea surface temperature of the model evolves with time during the courses of two time integrations of the model with normal ($1 \times CO_2$) and four times the normal ($4 \times CO_2$) concentration of CO_2. This figure clearly indicates that, in both experiments, the global mean sea surface temperature stops changing about 15 yr after the beginning of each time integration. In Section 4.4, the climatic effect of the increase in CO_2 concentration is discussed based upon analysis of the differences between the two statistically stationary states which emerge from the $1 \times CO_2$ and $4 \times CO_2$ experiments.

4.4. Thermal Response

4.4.1. Annual Mean Response. The latitude–height distribution of the CO_2-induced change of zonal mean, annually averaged temperature is illustrated in Fig. 8. In qualitative agreement with the results from the study of radiative, convective equilibrium described earlier, the temperature of the model troposphere increases whereas that of the model strato-

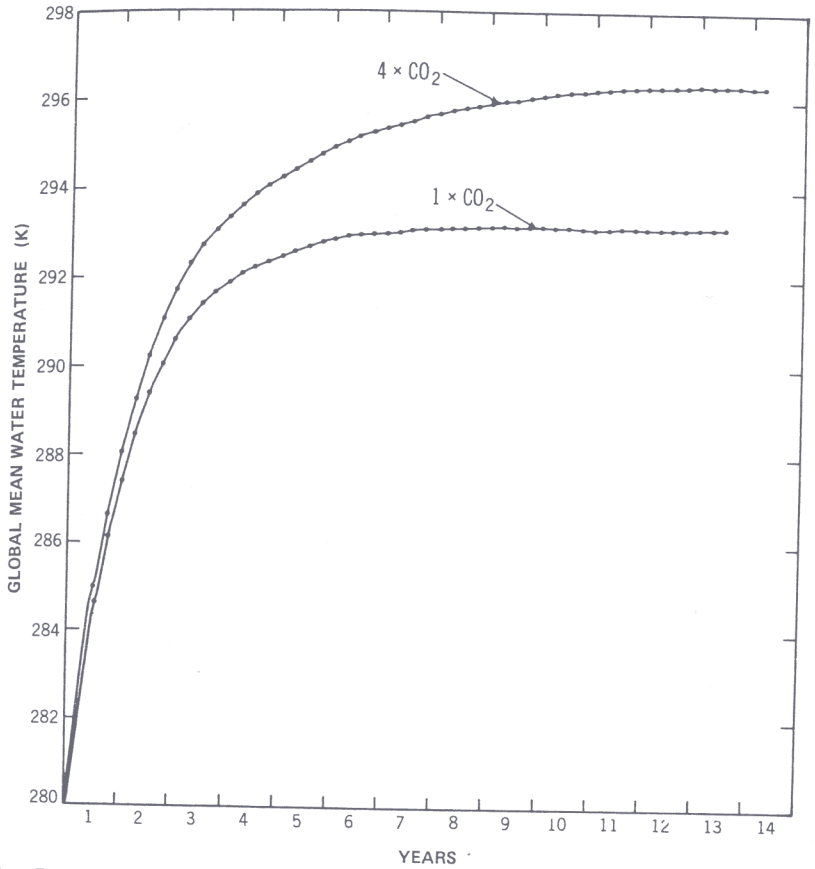

FIG. 7. Time variation of the global mean water temperature of ocean surface from the $1 \times CO_2$ and $4 \times CO_2$ experiments. (From Manabe and Stouffer, 1980.)

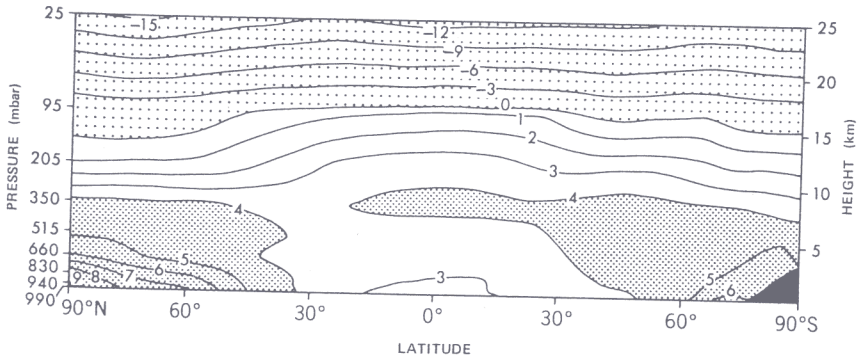

FIG. 8. Latitude–height distribution of the zonal mean difference in annual mean temperature (K) between the $4 \times CO_2$ and $1 \times CO_2$ model atmospheres. (From Manabe and Stouffer, 1980.)

sphere decreases in response to the increase of the CO_2 concentration in air. The tropospheric warming is particularly pronounced in the surface layer at high latitudes where the poleward retreat of snow cover and sea ice with high albedo enhances the warming. At low latitudes, the CO_2-induced heating spreads over the entire model troposphere via the effect of moist convection. Furthermore, the warming in the upper model troposphere is larger than the warming near the earth's surface because of the moist convective control of the vertical temperature distribution in low latitudes. (Note that the moist adiabatic lapse rate decreases with increasing air temperature.) Accordingly, the increase of surface air temperature at low latitudes is much less than the corresponding increase at high latitudes where the heating enhanced by the reduction of surface albedo is limited to the lower model troposphere due to stable stratification. The distribution of the annual mean response described above is qualitatively similar to the earlier results discussed by Manabe and Wetherald (1975, 1980).

One of the important factors which determines the sensitivity of surface temperature to the change of the atmospheric CO_2 concentration is the parameter B, defined by

$$B = \partial F / \partial T_s \tag{4.1}$$

where F is the outgoing terrestrial radiation at the top of the atmosphere and T_s is surface temperature. Because of the latitudinal variation of the vertical profile of the CO_2-induced warming in the model troposphere described in the preceding paragraph, the values of B at high latitudes are much smaller than the corresponding values at low latitudes. Therefore, in order to compensate for the decrease of F due to the CO_2-induced increase in the atmospheric opacity, the surface temperature at high latitudes must increase much more than the surface temperature at low latitudes. In short, the latitudinal variation of B discussed here partly accounts for the difference in the sensitivity of surface temperature between high and low latitudes, as pointed out by Held (1978).

Figure 8 also reveals that at high latitudes of the model, the lower tropospheric warming in the Northern Hemisphere is larger than the corresponding warming in the Southern Hemisphere. This interhemispheric difference in warming partly results from the absence of the snow albedo feedback mechanism over Antarctica covered by continental ice sheets. It should be kept in mind, however, that the simulated sea surface temperature is too high and the area coverage of sea ice is too narrow in the Southern Hemisphere of the model. Thus, this model tends to underestimate the effect of sea ice albedo feedback and, accordingly, the CO_2-

induced warming in the Southern Hemisphere. A better simulation of the sea ice distribution is required before one can discuss the interhemispheric asymmetry of the CO_2-induced warming.

Owing to the interhemispheric difference in the CO_2-induced warming discussed above, the area mean change of surface air temperature in the Northern Hemisphere is +4.5°C and is larger than the area mean warming of +3.6°C in the Southern Hemisphere. Thus, the global mean increase of surface air temperature is 4.1°C. This result suggests that the warming due to doubling of the CO_2 concentration would be about 2°C provided that the warming is proportional to the increase in the logarithm of the atmospheric CO_2 concentration as explained earlier. This is similar to the corresponding warming of 1.9°C obtained from the radiative, convective model of Manabe (1971) (see Fig. 1). In the global model atmosphere, the surface warming at high latitudes is enhanced by the albedo feedback mechanism and stable stratification, whereas the surface warming at low latitudes is reduced by moist convection as discussed earlier. Because of these two opposing influences, the area mean surface warming of the global model turns out to be similar to the surface warming of the one-dimensional model.

Table II contains the estimates of area mean increases of surface air temperatures (in response to the doubling of atmospheric CO_2 concentration) which were obtained by various authors from their general circulation models of climate. This table indicates that the magnitude of the warming obtained from the seasonal model of Hansen (1979) is 3.9°C and is significantly more than the warming of 2.0°C from the model of Manabe and Stouffer. Since the details of Hansen's study have not been published, it is difficult to determine the basic causes for the difference. According to the report of the Climate Research Board (1979), Hansen obtained larger warming partly because the positive feedback effect of snow cover is exaggerated in his model. In his standard ($1 \times CO_2$) experiment, the simulated surface air temperature is colder than the observed temperature and the area of snow cover is too extensive, resulting in the larger sensitivity mentioned above. In addition, it is speculated in the report that the difference in warming may also result from the difference in the treatment of cloud cover in the two models. Cloud cover is a prognostic variable in the Hansen model, whereas it is prescribed in the model of Manabe and Stouffer. Further comparative assessment of the two studies appears to be necessary before one can pinpoint the real cause of the difference between the results from these two studies.

It is significant that the estimates of the CO_2-induced warming obtained by Gates *et al.* (1981) and Mitchel (1979) are much smaller than the esti-

TABLE II. ESTIMATES FROM NUMERICAL MODEL EXPERIMENTS OF THE WARMING OF AREA-MEAN SURFACE AIR TEMPERATURE $\overline{\Delta T}^{A}$ (°C) RESULTING FROM DOUBLING OF CO_2 CONCENTRATION IN THE ATMOSPHERE

Reference	Geography	Sea surface temperature	Insolation	Cloud	$\overline{\Delta T}^{A}$ (°C) doubling
Interactive ocean					
Manabe and Wetherald (1975)	Idealized	Predicted	Annual	Prescribed	2.9
Manabe and Wetherald (1980)	Idealized	Predicted	Annual	Predicted	3.0
Wetherald and Manabe (1981)	Idealized	Predicted	Annual	Prescribed	3.0[a]
Wetherald and Manabe (1981)	Idealized	Predicted	Seasonal	Prescribed	2.4[a]
Manabe and Stouffer (1979, 1980)	Realistic	Predicted	Seasonal	Prescribed	2.0[a]
Hansen *et al.* (1979a)	Realistic	Predicted	Annual	Predicted	3.9
Hansen *et al.* (1979b)	Realistic	Predicted	Seasonal	Predicted	3.5
Noninteractive ocean					
Gates *et al.* (1981)	Realistic	Prescribed	Seasonal	Predicted	0.3
Mitchell (1979)	Realistic	Prescribed	Seasonal	Prescribed	0.2

[a] Temperature changes inferred from the results of numerical experiments in which the atmospheric CO_2 concentration is increased by a factor of four.

mates obtained from other studies. This is because they assumed that sea surface temperature is unaltered by the increase of the atmospheric CO_2 concentration, imposing a strong constraint upon the changes of the temperature of their model atmospheres.

Table II also reveals that a model with the seasonal variation of insolation is less sensitive to the increase of the atmospheric CO_2 concentration than another version of the model with an annual mean insolation. [Note the difference between the results from the annual and seasonal models of Hansen and the corresponding difference in the results of Wetherald and Manabe (1981).] This is partly because the contribution of the albedo feedback mechanism is smaller in a seasonal model in which snow cover is absent over the Northern Hemisphere continents during most of summer. For further discussion of this topic, refer to Wetherald and Manabe (1981).

Based upon the results from both one-dimensional models and general circulation models of climate, the report of the Climate Research Board (1979) concluded that the global mean increase of surface air temperature

resulting from the doubling of the atmospheric CO_2 concentration is near 3°C with a probable error of 1.5°C. In view of the difficulty in developing a reliable scheme of cloud prediction and a realistic model of the joint ocean–atmosphere system, it will take some time to reduce the uncertainty in the estimate of the CO_2-induced change in the atmospheric temperature.

4.4.2. Seasonal Response. Figure 9 shows the seasonal variation of the difference between the zonal mean surface air temperatures of the 4 × CO_2 and the 1 × CO_2 atmospheres. At low latitudes, the warming due to the quadrupling of the atmospheric CO_2 concentration is relatively small and depends little on season, whereas at high latitudes it is generally larger and varies markedly with season, particularly in the Northern Hemisphere. Over the Arctic Ocean and its vicinity, the warming is at a maximum in early winter and is small in summer. This implies that the range of seasonal variation of surface air temperature in these regions decreases significantly in response to the CO_2 increase.

An analysis of heat fluxes over the Arctic Ocean of the model indicates that the CO_2-induced reduction of sea ice thickness is mainly responsible for the large early winter warming of surface air mentioned above. In early winter, the upward conductive heat flux through sea ice in the 4 × CO_2 experiment is larger than the corresponding flux in the 1 × CO_2

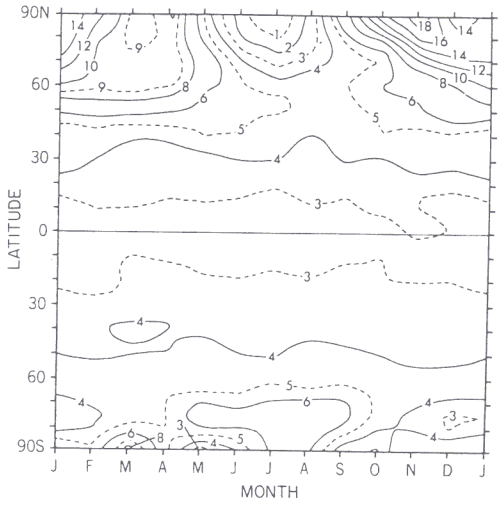

FIG. 9. Latitude–time distribution of the zonal mean difference in surface air temperature (K) between the 4 × CO_2 and 1 × CO_2 model atmospheres. (From Manabe and Stouffer, 1980.) Zonal averaging is made over both oceans and continents.

experiment because of the difference in sea ice thickness. Accordingly, the flux of sensible heat from the ice surface to the atmosphere in the former experiment is also larger than the corresponding flux in the latter experiment. This difference in the upward flux of sensible heat accounts for the large CO_2-induced warming of surface air in early winter. The winter warming is further enhanced by a stable stratification which limits the heating to the lowest layer of the model troposphere at high latitudes.

As Fig. 9 indicates, the magnitude of the warming in summer is much less than the corresponding warming in winter. Because of the reduction of sea ice, the surface albedo decreases significantly from the $1 \times CO_2$ to the $4 \times CO_2$ experiment. However, the additional energy of solar and terrestrial radiation absorbed by ocean surface is used either for melting the sea ice or warming the ice-free mixed-layer ocean which has a large heat capacity. Thus, the summer warming of surface air turns out to be relatively small. It should be noted, however, that the additional energy absorbed during summer in the $4 \times CO_2$ case, delays the appearance of sea ice or reduces its thickness, thereby increasing the conductive heat flux in early winter when the air–water temperature difference becomes very large.

The seasonal variation of the CO_2-induced warming of surface air temperature over the model continents is significantly different from the variation over the model oceans. According to Fig. 10, which shows the latitude–time distribution of the increase in zonal mean surface air temperature over continents, the CO_2-induced warming of high latitudes is at a maximum in early winter, being influenced by the large warming over the Arctic Ocean discussed above. However, Fig. 10 also indicates a secondary center of relatively large warming around 65° N in April. This results from a large reduction in surface albedo during spring when the insolation acquires a near-maximum intensity. The CO_2-induced reduction of snow cover area is responsible for this albedo change.

The discussion in the preceding paragraphs indicates that, as compared with snow cover, sea ice has a quite different influence on the seasonal variation of the CO_2-induced increase of surface air temperature at high latitudes. This is because sea ice not only reflects a large fraction of solar radiation, but also reduces the heat exchange between the atmosphere and underlying seawater. Thus, the CO_2-induced warming of surface air over the Arctic Ocean is at a maximum during early winter as discussed earlier. On the other hand, the warming over continents is also large in spring, when the heating due to the snow albedo feedback mechanism is largest.

In assessing the results of Manabe and Stouffer described here, it is desirable to keep in mind that the mixed layer of their model does not

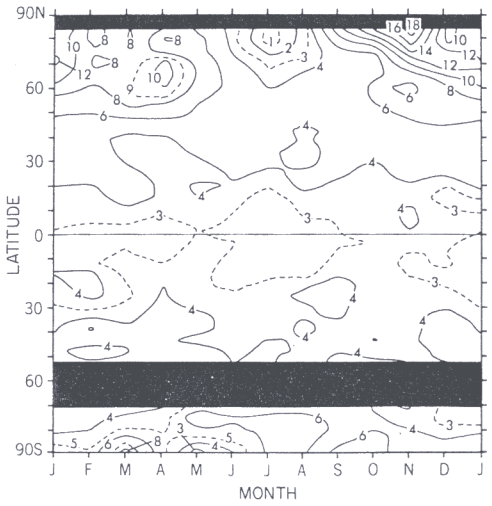

FIG. 10. Same as Fig. 9 except that the zonal averaging of surface air temperature is computed only over continents. (From Manabe and Stouffer, 1980.)

exchange heat with the deeper layer of ocean. Nevertheless, the qualitative aspect of their results is probably valid because a stably stratified halocline, which exists beneath the mixed layer of the Arctic Ocean, markedly reduces the heat exchange between the mixed layer and the deeper layer of the ocean.

4.4.3. Geographical Response. The geographical distribution of the difference between the annual mean surface air temperatures of the 4 × CO_2 and 1 × CO_2 atmospheres is shown in Fig. 11a. This figure indicates that the distribution of the CO_2-induced annual mean warming is almost zonal and reveals the characteristics which are identified in Section 4.4.2 on zonal mean response (i.e., large polar warming, relatively small warming in the tropics, and the interhemispheric asymmetry in the warming between the two polar regions).

The difference in the surface air temperature for the December–February (DJF) period is shown in Fig. 11b. According to this figure, the CO_2-induced warming is larger than its zonal average along the east coast of both Eurasian and North American continents. The large Arctic warming discussed in Section 4.4.2 reduces the cooling effect of the southward advection of cold air along the periphery of the Aleutian and Icelandic lows. This accounts for the relatively large CO_2-induced warming along the east coasts of continents mentioned above.

The distribution of the CO_2-induced change of surface air temperature

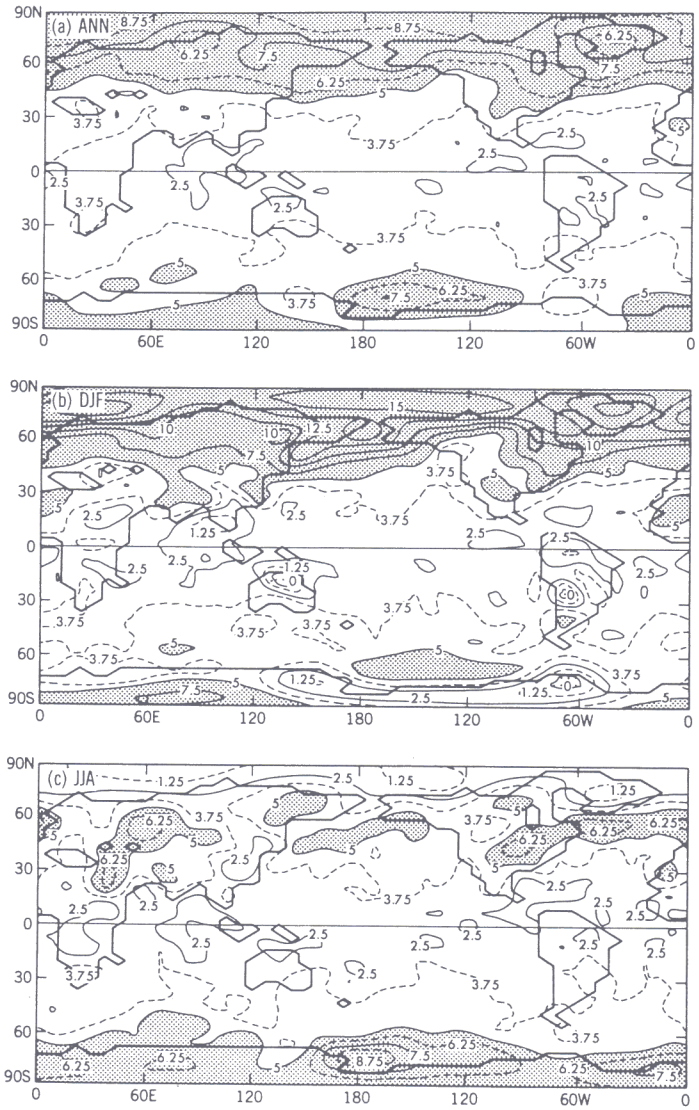

FIG. 11. Geographical distribution of the difference in surface air temperature (K) between the 4 × CO_2 and 1 × CO_2 model atmospheres: (a) annual mean difference; (b) December–January–February difference; (c) June–July–August difference. Shaded areas identify the regions where the difference exceeds 5°C. (From Manabe and Stouffer, 1980.)

for the June–August (JJA) period is shown in Fig. 11c. In this figure, one can identify the regions of relatively large warming over the continents at middle and high latitudes of the Northern Hemisphere. These regions approximately coincide with the regions where soil moisture decreases in response to the increase of the atmospheric CO_2. The reduction of soil moisture results in the reduction of evaporative ventilation and, accordingly, the warming of the continental surface, particularly during summer when the insolation is at or near maximum intensity. As will be discussed in Section 4.6.3, the geographical distribution of soil moisture change as determined by this numerical experiment is influenced by the large natural fluctuation of the model hydrology. Therefore, the details of the summer distribution of surface air temperature difference should be regarded with caution.

4.5. Hydrologic Response

4.5.1. Annual Mean Response. The increase in CO_2 concentration affects not only the thermal structure of the model atmosphere but also the hydrologic behavior of the model. One of the basic hydrologic changes is the overall intensification of the hydrologic cycle. In response to the quadrupling of the atmospheric CO_2 content, the global mean rates of both evaporation and precipitation increase by as much as 7%.

One of the important factors responsible for the intensification of the hydrologic cycle is the change in the surface radiation budget. For example, an increase in atmospheric CO_2 enhances the downward flux of terrestrial radiation reaching the earth's surface. In addition, the CO_2-induced warming of the troposphere results in the increase of absolute humidity as discussed in Section 3 and also contributes to the increase of downward flux of terrestrial radiation. Thus, a larger amount of radiative energy is received by the earth's surface, to be removed as turbulent fluxes of sensible and latent heat. This accounts for the increase in the global mean rate of evaporation mentioned above.

One can identify another important factor which is responsible for the enhancement of evaporation. According to the Clapeyron–Clausius relationship between the saturation vapor pressure and temperature, the saturation vapor pressure increases almost exponentially with a linear increase of surface temperature. Thus, when surface temperature is high, evaporation becomes a more effective means of ventilating the earth's surface as compared with the upward flux of sensible heat. Accordingly, a larger fraction of radiative energy received by the earth's surface is removed as latent heat rather than sensible heat. This implies the CO_2-induced increase in the evaporation rate.

To satisfy the balance requirement of water vapor in the model atmosphere, the increase in the global mean rate of evaporation discussed above should be matched by a similar increase in the global mean rate of precipitation. This explains why the global mean rates of both precipitation and evaporation increase in response to an increase of atmospheric CO_2 content. For further discussion of the physical mechanisms which are responsible for the CO_2-induced increase of the intensity of the hydrologic cycle, see the articles by Manabe and Wetherald (1975) and by Wetherald and Manabe (1975).

The global intensification of the hydrologic cycle is evident in Fig. 12, which illustrates the latitudinal distributions of annually averaged, zonal mean rates of precipitation and evaporation from both the $1 \times CO_2$ and the $4 \times CO_2$ experiments. This figure indicates that at high latitudes, the increase of the precipitation rate is much larger than that of the evaporation rate, whereas the former tends to be smaller than the latter at low latitudes of the model. This result implies that, as compared with the $1 \times CO_2$ atmosphere, the $4 \times CO_2$ atmosphere receives more moisture from the earth's surface at low latitudes and returns it to high latitudes in the form of increased precipitation. The poleward transport of moisture in the model atmosphere increases significantly in response to the increase of atmospheric CO_2 and compensates for the difference in moisture exchange between the earth's surface and the atmosphere of the model as described above. The increase in the moisture content of air resulting from the CO_2-induced warming of the model troposphere accounts for the increase of poleward moisture transport as discussed by Manabe and Wetherald (1980). The increase of the precipitation rate at high latitudes is responsible for the enhanced wetness of soil over the Arctic and subarctic region during most of the year as discussed below.

4.5.2. Seasonal Response. The CO_2-induced change in the hydrology of the model has a significant seasonal dependence. Figure 13 illustrates the latitude–time distribution of the difference in zonal mean soil moisture between the $4 \times CO_2$ and $1 \times CO_2$ experiment. According to this figure, the difference in zonal mean soil moisture in high latitudes of the model has a large positive value throughout most of the year with the exception of the summer season. As discussed above, this CO_2-induced increase in soil moisture results from the penetration of warm, moisture-rich air into high latitudes of the model. Figure 13 also indicates two zones of reduced soil wetness at middle and high latitudes during the summer season. Qualitatively similar results were obtained by Wetherald and Manabe (1981) from a model with an idealized geography. The characteristics of the CO_2-induced change of soil moisture identified above have relatively high statistical significance (Manabe *et al.*, 1981; Hayashi, 1982).

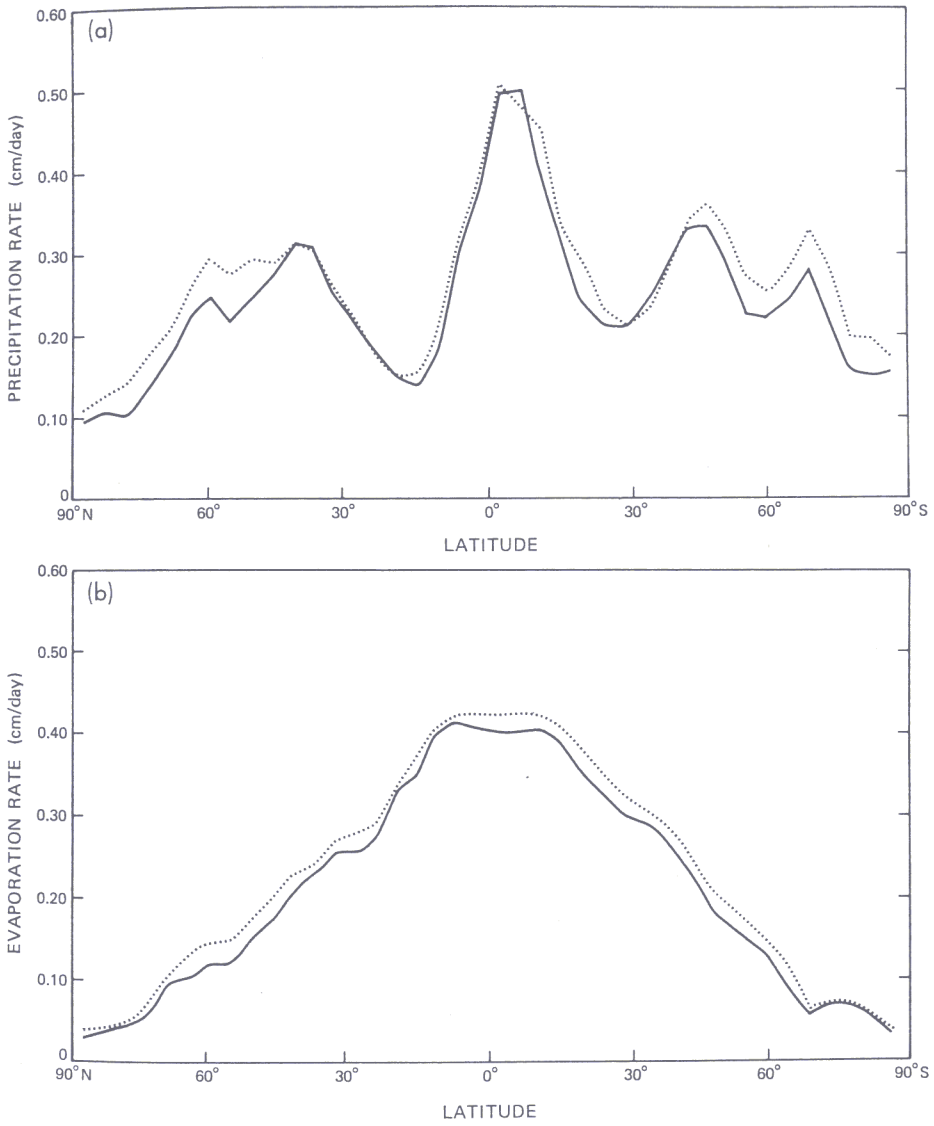

FIG. 12. Latitudinal distribution of (a) zonal mean precipitation rate and (b) zonal mean evaporation rate (in units of centimeters per day) from the 4 × CO_2 (·····) and 1 × CO_2 (——) experiments. (From Manabe and Stouffer, 1980.)

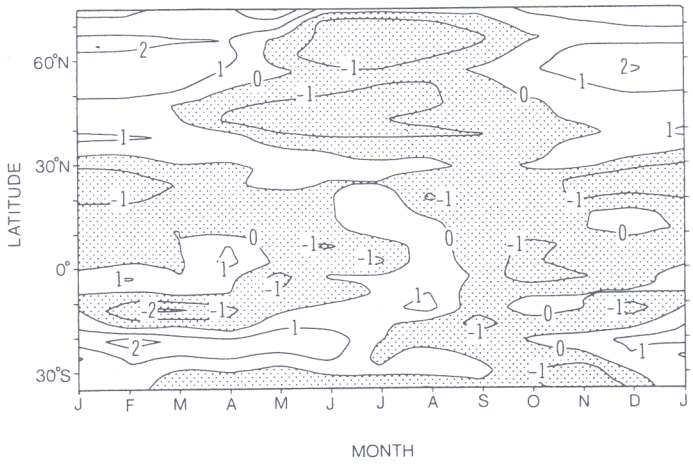

FIG. 13. Latitude–time distribution of zonal mean difference in soil moisture (cm) over continents between the 4 × CO_2 and 1 × CO_2 experiments. Note that the field capacity of soil moisture is assumed to be 15 cm everywhere. The zonal mean difference is not shown in high-latitude regions of both hemispheres where the longitudinal span of continents is either zero or very small. (From Manabe and Stouffer, 1980.)

To appreciate the relative magnitude of the CO_2-induced soil moisture change, the percentage change of soil moisture is computed by averaging the results from two sets of CO_2 sensitivity experiments and is shown in Fig. 14. This figure indicates that during summer the percentage reduction of zonal mean soil moisture exceeds 20% at 60° N and 44° N. The percentage increase of zonal mean soil moisture, which occurs at high latitudes except during summer, exceeds 10%. In short, the changes in zonal mean soil moisture described in the preceding paragraph, constitute a substantial fraction of the amount of soil moisture itself. Another feature of interest in Fig. 14 is a large fractional reduction of zonal mean soil moisture at about 25° N in winter. Although one notes some fractional changes of zonal mean soil moisture in tropics of the model, the changes have relatively small statistical significance as compared with the changes at middle and high latitudes as discussed by Manabe *et al.* (1981) and Hayashi (1982).

To determine the mechanisms responsible for the CO_2-induced summer dryness at middle and high latitudes described above, Manabe *et al.* (1981) made an extensive analysis of the seasonal variation of the soil moisture budget from the model. Their analysis reveals that at high latitudes, the snowmelt season in the 4 × CO_2 experiment ends earlier than the corresponding season in the 1 × CO_2 experiment. Thus, the warm season of rapid soil moisture depletion begins earlier due to enhanced evaporation, resulting in less soil moisture during summer in the 4 × CO_2

experiment. The mechanism described above is mainly responsible for the CO_2-induced dryness in summer at high latitudes of the model.

At middle latitudes, the earlier timing of the spring maximum in snowmelt also contributes to the summer dryness as at high latitudes. In addition, the spring-to-summer reduction in the precipitation rate occurs earlier, contributing to the earlier beginning of the drying season and CO_2-induced summer dryness. In the $4 \times CO_2$ experiment, the period of weak baroclinicity during summer begins earlier than the standard experiment, resulting in the earlier occurrence of the spring-to-summer reduction in the precipitation rate mentioned above.

One can identify another factor which is responsible for the earlier occurrences of the spring maximum and of the spring-to-summer reduction of the precipitation rate. In a CO_2-rich atmosphere, the middle-latitude rainbelt is located poleward of the corresponding rainbelt in the normal CO_2 atmosphere because of the penetration of the moisture-rich, warm air into high-latitude regions. Since the middle-latitude rainbelt moves poleward from winter to summer, this poleward shift of the rainbelt implies an earlier arrival of the rainbelt in spring. It also accounts for the CO_2-induced winter dryness in the model subtropics mentioned above.

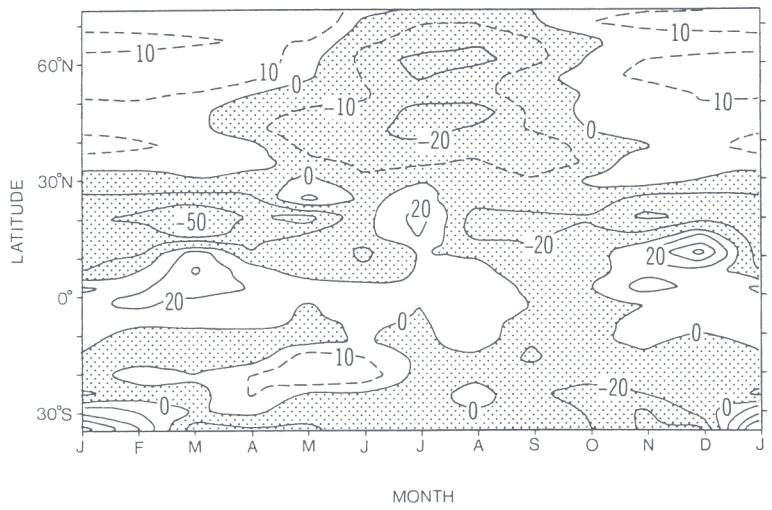

FIG. 14. Latitude–time distribution of the percentage change in zonal mean soil moisture over continents in response to the quadrupling of the atmospheric CO_2 concentration. Here, the percentage of difference is computed by averaging the results from two versions of the global model with two different computational resolutions. The zonal mean difference is not shown in high-latitude regions of both hemispheres where the longitudinal span of continents is either zero or very small. See Manabe *et al.* (1981) for further details.

4.5.3. Geographical Distribution. So far, the CO_2-induced change of zonal mean soil moisture has been discussed. However, one of the ultimate goals of the CO_2–climate sensitivity study is the determination of the geographical distribution of the climate change. Manabe *et al.* (1981) made a preliminary attempt to evaluate the geographical distribution of the CO_2-induced change of soil moisture. Unfortunately, the local hydrology of a general circulation model has much larger temporal variability than the zonal mean hydrology. In order to distinguish the CO_2-induced local hydrologic change from the natural fluctuation of the model hydrology, it is necessary to perform a very long-term integration of the model. The periods of the numerical time integrations conducted by Manabe *et al.* are too short for this purpose. Furthermore, the geographical distribution of hydrologic variables (i.e., precipitation rate) as simulated by current climate models contains many unrealistic features. Therefore, the geographical details of the CO_2-induced hydrologic change is a topic for future studies.

4.6. Signal-to-Noise Ratio[2]

In Sections 4.4 and 4.5, the distribution of the CO_2-induced change in a global model climate is discussed. To appreciate the practical implications of such a climate change and assess its detectability, it is desirable to compare the CO_2-induced change with the magnitude of natural fluctuation of climate. For this purpose, one can estimate the signal-to-noise ratio S/N for the CO_2-induced change of a climatic variable from the following equation:

$$S/N = \Delta_c q/\tilde{\sigma}_q \tag{4.2}$$

where $\Delta_c q$ indicates the CO_2-induced change of a variable q and $\tilde{\sigma}_q$ denotes a weighted mean standard deviation of q defined by

$$\tilde{\sigma}_q = \frac{(N^{1c} - 1)\sigma_q^{1c} + (N^{4c} - 1)\sigma_q^{4c}}{(N^{1c} - 1) + (N^{4c} - 1)} \tag{4.3}$$

Here, σ_q^{1c} and σ_q^{4c} are the standard deviations of q in the $1 \times CO_2$ and $4 \times CO_2$ experiments, respectively. N^{1c} and N^{4c} are the number of samples (i.e., number of years in the analysis period) from the two experiments (10 and 3, respectively).

When the signal-to-noise ratio as defined above is much larger than 1,

[2] The results described in this section have not been previously published. They are obtained through a recent collaboration between S. Manabe and R. J. Stouffer.

the CO_2-induced change in q is much larger than the magnitude of its natural fluctuation and can easily be detected. On the other hand, if the signal-to-noise ratio is much less than unity, it is practically impossible to detect the CO_2-induced change because it is obscured by the natural variation. In this situation, the CO_2-induced change has little practical implication.

The signal-to-noise ratio is computed for the monthly averaged, zonal mean values of surface air temperature and soil moisture which are discussed in the preceding sections. For this purpose, the periods of the $1 \times CO_2$ and $4 \times CO_2$ time integrations are extended to year 20 and year 16, respectively (see Fig. 7). The data from the last 10-year and 3-year periods of the two time integrations are used for this analysis.

Figure 15a illustrates the latitudinal and seasonal variation of the signal-to-noise ratio for the CO_2-induced change of zonal mean surface air temperature over continents (see Fig. 10 for the distribution of the signal). According to this figure, the signal-to-noise ratio of this quantity in middle latitudes of the Northern Hemisphere is at a maximum during summer when the natural variability of surface air temperature is relatively small. Although the CO_2-induced change of surface air temperature is particularly large at high latitudes with the exception of summer season, the distribution of the signal-to-noise ratio does not share the similar characteristics because the temporal fluctuation of zonal mean surface air temperature is very large near the poles. Earlier, Wigley and Jones (1981) obtained a qualitatively similar result from the CO_2-induced signal shown in Fig. 10 and the observed variability of surface air temperature in the real atmosphere. (See Fig. 1 of their paper. One can approximately deduce the signal-to-noise ratio defined here by dividing their version of signal-to-noise ratio by $\sqrt{5}$.) The similarity between the two results implies that the noise level of the model is not very different from the noise level in the actual atmosphere as determined by Wigley and Jones. In the Southern Hemisphere, where the latitudinal span of continents is narrow, the signal-to-noise ratio over continents is small because of high noise level. Although it is not shown here, the signal-to-noise ratio of zonally averaged surface air temperature over oceans is much larger than the corresponding ratio over continents due to the small variability of surface air temperature over oceans.

The signal-to-noise ratio for zonal mean surface air temperature over both oceans and continents is illustrated in Fig. 15b. In the Northern Hemisphere, the signal-to-noise ratio is large in middle latitudes during the summer season as it is over continents. In the Southern Hemisphere, it is relatively large in middle latitudes throughout most of the year. The signal-to-noise ratio is relatively small in the polar regions where the

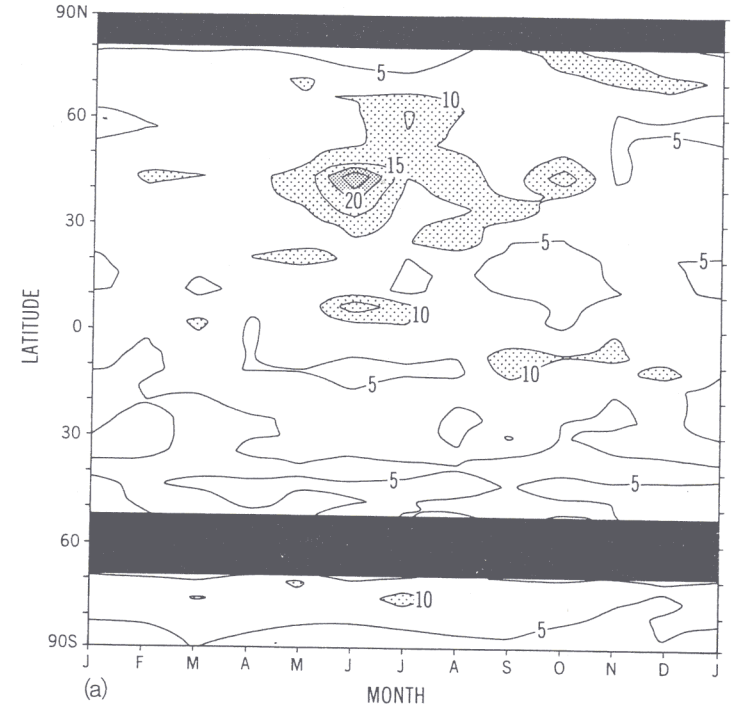
90N
60
30
0
30
60
90S
LATITUDE
5
10
15
20
J F M A M J J A S O N D J
MONTH
(a)

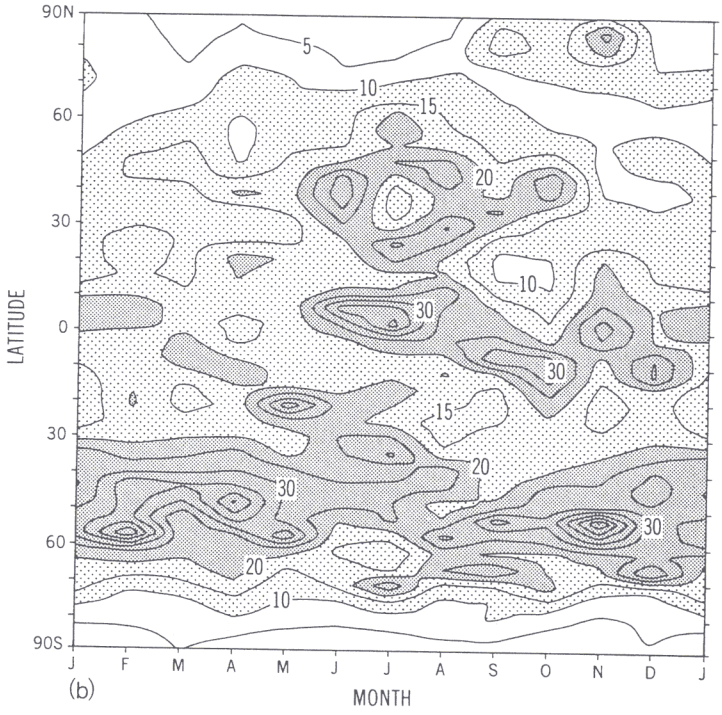
90N
60
30
0
30
60
90S
LATITUDE
5
10
15
20
30
J F M A M J J A S O N D J
MONTH
(b)

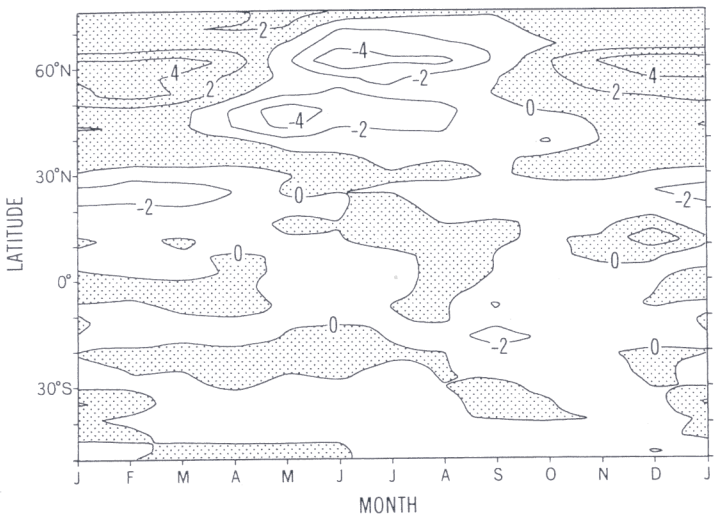

FIG. 16. The latitude–time distribution of the signal-to-noise ratio for the change of zonally averaged, monthly mean soil moisture over continents in response to the quadrupling of the atmospheric CO_2 concentration.

variability of zonally averaged surface air temperature is particularly large, as discussed by North *et al.* (1982).

Figure 16 illustrates the latitudinal and seasonal variation of the signal-to-noise ratio for the CO_2-induced change in zonal mean soil moisture over continents. (See Fig. 13 for the distribution of the signal.) According to this figure, some of the features with relatively large signal-to-noise ratio include the enhanced summer dryness in middle and high latitudes of the Northern Hemisphere, the enhanced winter dryness around 25° N, and the enhanced wetness around 60° N during the fall–winter–spring period. (In the Southern Hemisphere, the signal-to-noise ratio is small because the longitudinal span of continents is small.) Figure 16 also indicates that the changes of soil moisture, which are caused by the quadrupling (or doubling) of atmospheric CO_2 may have a magnitude comparable to its natural variability. Comparison of Figs. 15a and 16 reveals that the signal-to-noise ratio of this variable is much less than the corresponding ratio for the surface air temperature. In summary, the results from the present study suggest that it is harder to detect the CO_2-induced change in soil moisture than the corresponding change in surface air temperature.

FIG. 15. The latitude–time distribution of the signal-to-noise ratio for the change of zonally averaged, monthly mean surface air temperature in response to the quadrupling of the atmospheric CO_2 concentration. The zonal averaging is made over (a) continents and (b) both oceans and continents.

[The statistical significance of the CO_2-induced change may be evaluated by use of the signal-to-noise ratio obtained here. If the signal-to-noise ratio in Figs. 15 and 16 is equal to 1.45, the change is statistically significant at 95% confidence level. For a discussion of the Student's t test, see the book by Panofsky and Brier (1968).]

5. Transient Response

In Section 4, the discussions focused upon the difference between the two equilibrium climates of a model with normal and above-normal atmospheric CO_2 concentrations. However, this equilibrium response of climate will not be realized immediately mainly because of the large thermal inertia of oceans. Therefore, it is important to determine the features of the transient response of climate resulting from the future increase of atmospheric CO_2.

Preliminary studies of CO_2-induced transient climate change have been conducted by the use of simple energy balance models of the ocean–atmosphere system (Schneider and Thompson, 1981; Hoffert *et al.*, 1980). Based upon the results from their study, Schneider and Thompson suggested that the latitudinal distribution of the transient change of climate may be quite different from the equilibrium response described in the preceding sections. For a further investigation of this problem, it is desirable to develop a comprehensive model of the ocean–atmosphere system.

Since the atmosphere–mixed-layer ocean model described in Section 4 lacks the deeper layers of an ocean which have large heat capacity, it is not suitable for the transient response study mentioned above. In order to investigate this problem, it is necessary to construct a full ocean–atmosphere model in which general circulation models of the atmosphere and a full ocean model are coupled with each other. Such a model has been developed at the Geophysical Fluid Dynamics Laboratory during the last 15 yr (Manabe and Bryan, 1969; Manabe *et al.*, 1979). Recently, Bryan *et al.* (1982) used a simplified version of the model for a study of the CO_2 transient response problem. Because of the many assumptions and simplifications adopted in the construction of the model, the quantitative aspect of the result should be received with caution. Nevertheless, the results from this study yield some preliminary insight into the nature of this problem. A brief description of this study follows.

5.1. *Coupled Ocean–Atmosphere Model*

As pointed out already, major simplification and idealization are incorporated into the coupled ocean–atmosphere model used in this prelimi-

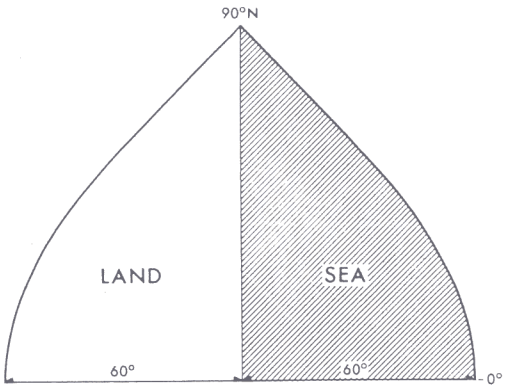

FIG. 17. Computational domain of the ocean–atmosphere model (Bryan *et al.*, 1982).

nary study. For example, seasonal variation of solar insolation is not included, and the geometry of land and sea is highly idealized as shown in Fig. 17. To minimize the amount of calculation, the model atmosphere and ocean are constrained to be triply periodic in the zonal direction with mirror symmetry across the equator. The basic structure of the model is illustrated in Fig. 18 as a box diagram.

The atmospheric component of the model is identical to that of the atmosphere–mixed-layer ocean model used for the study described in Section 4.2 (with the exception of simplifications identified in the preceding paragraph). The oceanic component of the model does not have a sufficient horizontal resolution to simulate mesoscale eddies, which are the dynamic counterparts of cyclones and anticyclones in the atmo-

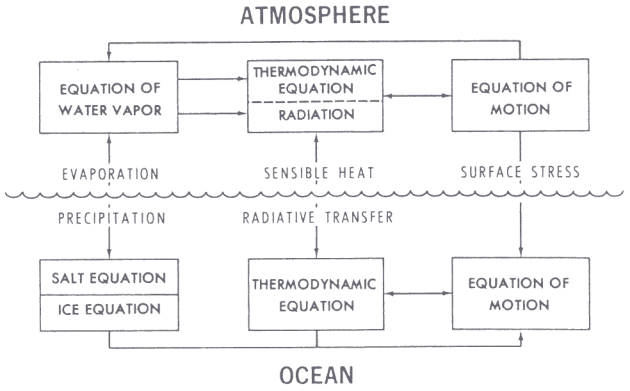

FIG. 18. Box diagram illustrating the structure of the ocean–atmosphere model (Manabe and Bryan, 1969).

sphere. The resolution is sufficient, however, to include the main features of the observed wind-driven and thermohaline circulation. A simple model of sea ice and land snow cover is incorporated as described in Section 4.2.

5.2. *Design of Switch-On Experiment*

Since the main topic of this study is the response of the coupled model as it makes the transition from one equilibrium state to another, the first requirement was to calculate equilibrium climates corresponding to the normal and above-normal atmospheric CO_2 concentrations. In order to obtain a climatic equilibrium of the model, it was necessary to use an economical method of numerical time integration developed by Manabe and Bryan (1969), Bryan and Lewis (1979), and Manabe *et al.* (1979) because it takes an extremely long time (several thousand years) for the coupled system to reach a statistically stationary equilibrium climate. This method, which is called the "nonsynchronous method," may be thought of as a relaxation procedure to hasten the convergence to equilibrium. In this study, 1 yr in the atmosphere model was taken to correspond to 110 yr in the upper ocean. One year in the upper ocean, in turn, was taken to be equivalent to 25 yr in the deepest level of the ocean.

The determination of two climatic equilibrium states provides the basis for a switch-on experiment in which the normal CO_2 equilibrium climate is perturbed by a sudden quadrupling of the atmospheric CO_2 concentration. The atmospheric and oceanic components of the model are time-integrated over a period of 25 yr in a synchronous mode as opposed to the nonsynchronous, economical method used to obtain a climate equilibrium.

5.3. *Temporal Variation*

Figure 19 illustrates the zonally averaged response at the 10th year of the time integration. The atmosphere exhibits the largest response at low levels near the pole, whereas the temperature of the underlying ice-covered seawater hardly changes (i.e., remaining at the freezing point). This result indicates that sea ice insulates the surface air from the underlying seawater. Around the sea ice margin, i.e., at about 75° N, the warming of the sea surface temperature is limited to the surface layer of the water because of a stably stratified halocline which insulates the shallow surface layer from the deeper layers of the ocean. The deepest penetration of the

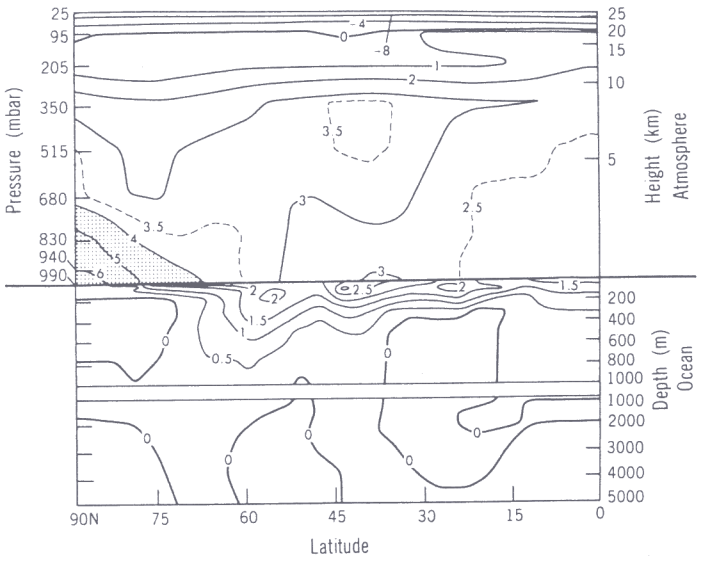

FIG. 19. Latitude–height distribution of zonally averaged temperature of the ocean–atmosphere model at the 10th year minus initial temperature (K), showing the response to a step function increase in atmospheric CO_2 (Bryan *et al.*, 1982).

heat anomaly occurs at about 60° N, where the stratification of the ocean is relatively weak and convective overturning occurs frequently. The greater stratification of the tropical ocean accounts for the smaller penetration of the heat anomaly at low latitudes.

To evaluate the response of the model atmosphere in comparison with its equilibrium response, the change of surface air temperature T may be normalized as follows:

$$R = (T - T_0)/(T_\infty - T_0) \tag{5.1}$$

where R is the normalized response; T_0 and T_∞ are the initial and final values of the surface air temperature, respectively. T_0 and T_∞ are equal to the equilibrium surface air temperatures of the model atmospheres with the normal and above-normal concentrations of CO_2, respectively. The zonal mean values of R are computed separately over oceans and continents, and are illustrated as a function of latitude and time in Fig. 20a and b. According to Fig. 20a, the rise in surface air temperature over the oceans is initially more rapid at low latitudes than at 60° latitude, where the downward penetration of the heat anomaly is deeper. However, the normalized response becomes nearly uniform at all latitudes and is about 65% at about the 20th year of the time integration. This result suggests

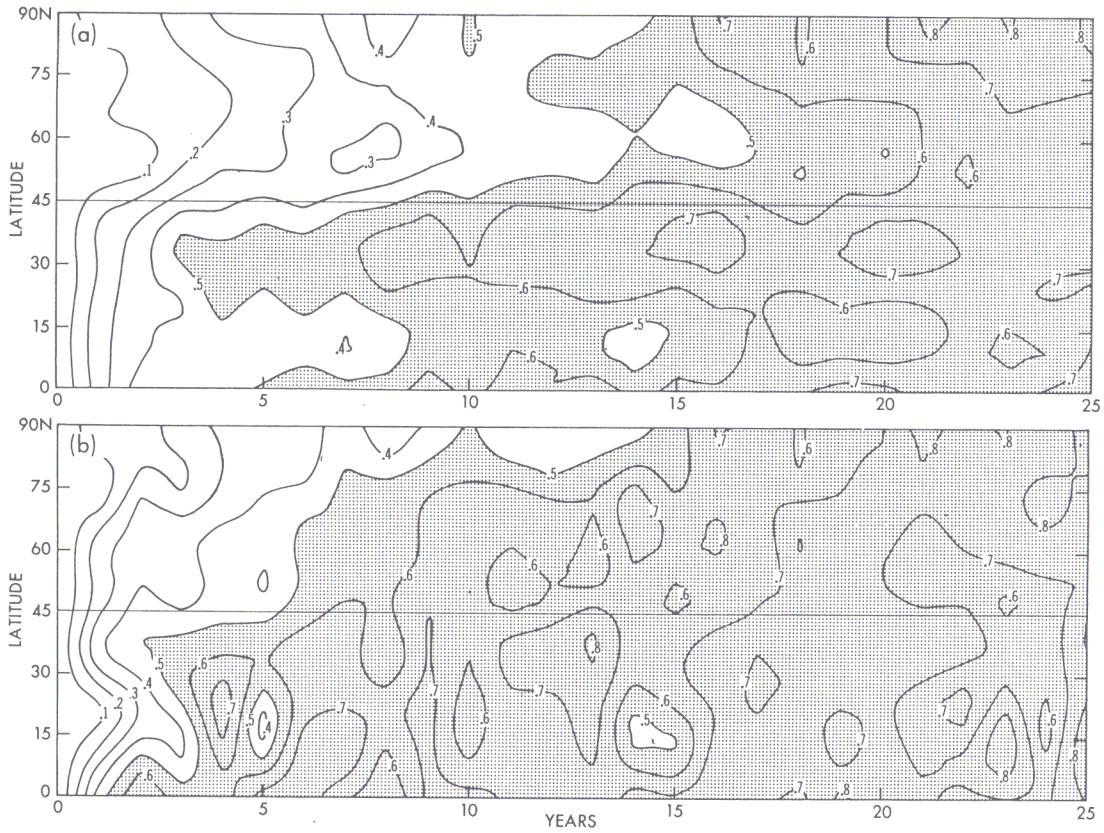

FIG. 20. Latitude–time variation of the zonally averaged normalized response R of surface air temperature over (a) oceans and (b) continents (Bryan *et al.* 1982). The normalized zonal mean response is $([T] - [T_0])/([T_\infty] - [T_0])$, where square brackets denote zonal mean operator.

that beyond the 20th year, the penetration of the heat anomaly into the deeper ocean is very slow and hardly influences the latitudinal profile of the normalized response of surface air temperature. Over the model continents which have zero thermal inertia, the normalized response of zonal mean surface air temperature is even faster and becomes nearly uniform as early as the 10th year (see Fig. 20b).

This result suggests that the latitudinal dependence of the transient response of surface air temperature is very similar to that of the equilibrium response provided that the time scale for the increase of the atmospheric CO_2 concentration is longer than ~10–20 years.

In view of many simplifications and shortcomings of the coupled model used for this study, the results from this computation must be regarded as tentative. Nevertheless, the study of Bryan *et al.* seems to indicate that, barring an unseen drastic acceleration of the rate of increase of atmospheric CO_2, sensitivity studies of climate equilibrium may be used as an approximate guide for predicting the latitudinal pattern of surface air temperature change in response to a gradual increase of atmospheric CO_2.

6. Concluding Remarks

In this presentation, I have reviewed some of the CO_2–climate sensitivity studies which have been conducted by various authors, in particular, by the staff members at the Geophysical Fluid Dynamics Laboratory of the NOAA. Based upon the results from mathematical models of climate with various degrees of complexities, it has been possible to identify the changes of climate resulting from an increase of atmospheric CO_2 content and to discuss the physical mechanisms responsible for the changes. Some of these CO_2-induced changes of climate are listed below.

(1) The temperature of the troposphere increases whereas that of the stratosphere decreases.
(2) The annual mean warming of the surface air at high latitudes is two to three times as large as the corresponding warming at low latitudes.
(3) Over the Arctic Ocean and the surrounding regions, the CO_2-induced warming has a large seasonal dependence. It is at a maximum in winter and at a minimum in summer. The warming has little seasonal dependence at low latitudes.
(4) The global mean rates of both precipitation and evaporation increase.
(5) The coverage and thickness of sea ice in the polar regions decrease.

(6) The snowmelt season arrives earlier.
(7) The annual mean rate of runoff increases at high latitudes.
(8) During summer, the zonal mean value of soil moisture in the Northern Hemisphere reduces in two belts of middle and high latitude, respectively.

The CO_2-induced changes of climate listed above have been identified by comparing two equilibrium climates of a mathematical model with normal and above-normal atmospheric CO_2 concentrations, respectively. Therefore, these changes may be qualitatively different from the transient response of climate to an increase of the atmospheric CO_2 concentration. In this presentation, I have also reviewed the results from a study in which the transient response of climate to a sudden increase of atmospheric CO_2 was investigated by the use of an ocean–atmosphere model with an idealized geography. The results from this preliminary study suggest that the latitudinal distribution of climate change from an equilibrium response study may be qualitatively similar to the transient response of climate, unless the CO_2 increase accelerates much faster than expected.

In order to make reliable assessments of both the equilibrium and the transient responses of climate to the future increase of atmospheric CO_2, it is necessary to further improve various components of the ocean–atmosphere model, in particular the oceanic component. For example, the thermocline as simulated by a current ocean model is too deep at low latitudes. Therefore, it is probable that a sensitivity study with a current model may yield a distorted assessment of the transient response of climate. Recent measurements of transient tracers such as tritium in the oceans provide data which are very suitable for validation of the transient behavior of ocean models. Preliminary studies of this kind have already been started by Sarmiento (1982).

Although the development of the atmospheric component of the model is at a more advanced stage than the oceanic component, it also has many shortcomings. For example, the geographical distributions of hydrologic variables (i.e., precipitation rate) as simulated by a current general circulation model of the atmosphere contain many unrealistic features, particularly in the vicinity of major mountain ranges (i.e., the Rockies, Himalayas, and Andes). This suggests that the dynamical computation of the flow over and around these mountain ranges requires further improvements.

In the global model described here, the distribution of cloud cover is prescribed. Accordingly, use of this global model implies the assumption

that cloud cover is unaltered by change in atmospheric CO_2. Although the success of the global model in simulating the seasonal variation of hemispheric mean values of radiative fluxes and surface air temperature encourages the author to believe that cloud cover may not have a dominant influence on the sensitivity of the global mean climate, it is far from obvious that this is the case (Smagorinsky, 1977). This is the subject of active debate in the current literature (Cess, 1976; Ohring and Clapp, 1980). The development of a reliable scheme of cloud cover prediction to be incorporated into a climate model is urgently needed for the study of this critical problem.

The CO_2-induced climate change described in this study has not been identified by observation mainly because such a change is obscured by the change of climate caused by other factors. These factors include the nonlinear interaction between the atmosphere and oceans, the long-term variation of solar luminosity, and the changes in the concentrations of aerosol and other minor atmospheric constituents (i.e., nitrous oxide, chrolofluorocarbon, etc.). Recently, Hansen *et al.* (1981) claimed to have detected the CO_2-induced climate change by separating the portion of the change attributable to some of these factors from the observed change of climate. However, a more careful determination of the contributions of these factors is required before one is convinced of the validity of their conclusion. For this purpose, it is necessary to carefully monitor the solar constant, the atmospheric loading of aerosols, and the spectral distributions of solar and terrestrial radiation fluxes at the top and bottom of the atmosphere. It is clear that the successful assessment of the CO_2-induced climate change requires an evenhanded emphasis upon both modeling research and monitoring of the climate-controlling parameters.

Acknowledgments

It is a pleasure to acknowledge the major contribution of Mr. R. T. Wetherald, who has collaborated with the author on the CO_2–climate sensitivity study during the past 20 years. Dr. J. Smagorinsky, the Director of the Geophysical Fluid Dynamics Laboratory, instigated and has wholeheartedly supported this long-term project. His foresight and leadership have been indispensable for the success of the project. The author is very grateful to Mr. R. J. Stouffer, Dr. K. Bryan, and Mr. M. J. Spelman with whom he conducted the very fruitful and enjoyable studies described in this review. Prof. J. Peixóto kindly persuaded the reluctant author to write this review. Drs. H. Levy II and J. Sarmiento reviewed the earlier version of the manuscript and made many valuable suggestions for its improvement. Finally, the assistance of Ms. J. Kennedy and Messrs. P. Tunison and J. Conner has been essential for the preparation of the manuscript.

References

Arrhenius, S. (1896). On the influence of carbonic acid in the air upon the temperature of the ground. *Philos. Mag.* [5] **41,** 237–276.

Augustsson, T., and Ramanathan, V. (1977). A radiative, convective model study of the CO_2 climate problem. *J. Atmos. Sci.* **34,** 448–451.

Bryan, K., and Lewis, L. J. (1979). A water mass model of the world ocean. *JGR, J. Geophys. Res.* **84**(C3), 2503–2517.

Bryan, K., Komro, F. G., Manabe, S., and Spelman, M. J. (1982). Transient climate response to increasing atmospheric CO_2. *Science* **215,** 56–58.

Callendar, G. S. (1938). The artificial production of carbon dioxide and its influence on temperature, *Q. J. R. Meteorol. Soc.* **64,** 223–240.

Cess, R. D. (1976). Climate change: An appraisal of atmospheric feedback mechanisms employing zonal climatology. *J. Atmos. Sci.* **33,** 1831–1843.

Climate Research Board (1979). "Carbon Dioxide and Climate: A Scientific Assessment." Nat. Acad. Sci., Washington, D.C.

Crutcher, H. L., and Meserve, J. M. (1970). "Selected Level Heights, Temperature, and Dew Points for the Northern Hemisphere," NAVAIR 50-IC-52. U.S. Nav. Weather Ser., Washington, D.C.

Ellis, J. S., and Vonder Haar, T. H. (1976). "Zonal Average Earth Radiation Budget Measurement from Satellite for Climate Studies," Atmos. Sci. Pap. 240. Colorado State University, Fort Collins.

Gates, W. L., Cook, K. H., and Schlesinger, M. (1981). Preliminary analysis of experiments on the climatic effects of increasing CO_2 with the OSU atmospheric general circulation model. *JGR, J. Geophys. Res.* **86**(C7), 6385–6393.

Geophysics Study Committee (1977). "Energy and Climate." Nat. Acad. Sci., Washington, D.C.

Hansen, J. E. (1979). "Proposal for Research in Global Carbon Dioxide Source/Sink Budget and Climate Effects." Goddard Institute for Space Studies, New York.

Hansen, J. E., Johnson, D., Lacis, A., Lebedeff, S., Lee, P., Rind, D., and Russel, G. (1981). Climatic impact of increasing atmospheric carbon dioxide. *Science* **213,** 957–966.

Hayashi, Y. (1982). Confidence interval of a climate signal. *J. Atmos. Sci.* **39,** 1895–1905.

Held, I. M. (1978). The tropospheric lapse rate and climate sensitivity experiments with a two-level atmospheric model. *J. Atmos. Sci.* **35,** 2083–2098.

Hoffert, M. I., Callegari, A. J., and Hsieh, C. T. (1980). The role of deep sea heat storage in the secular response to climatic forcing. *JGR, J. Geophys. Res.* **85,** 6667–6679.

Kaplan, L. D. (1960). The influence of carbon dioxide variation on the atmospheric heat balance. *Tellus* **12,** 204–208.

Kondratiev, K. Y., and Niilisk, H. I. (1960). On the question of carbon dioxide heat radiation in the atmosphere. *Geofis. Pura Appl.* **46,** 216–230.

Manabe, S. (1971). Estimates of the future changes of climate due to increase of carbon dioxide concentration in the air. *In* "Man's Impact on the Climate" (W. H. Matthews, W. W. Kellogg, and G. D. V. Robinson, eds.), pp. 249–264. MIT Press, Cambridge, Massachusetts.

Manabe, S., and Bryan, K. (1969). Climate calculation with a combined ocean-atmospheric model. *J. Atmos. Sci.* **26,** 786–789.

Manabe, S., and Stouffer, R. J. (1979). A CO_2-climate sensitivity study with a mathematical model of the global climate. *Nature (London)* **282,** 491–493.

Manabe, S., and Stouffer, R. J. (1980). Sensitivity of a global model to an increase of CO_2 concentration in the atmosphere. *JGR, J. Geophys. Res.* **85**(C10), 5529–5554.

Manabe, S., and Wetherald, R. T. (1967). Thermal equilibrium of the atmosphere with a given distribution of relative humidity. *J. Atmos. Sci.* **24,** 241–259.

Manabe, S., and Wetherald, R. T. (1975). The effects of doubling the CO_2-concentration on the climate of a general circulation model. *J. Atmos. Sci.* **32,** 3–15.

Manabe, S., and Wetherald, R. T. (1980). On the distribution of climate change resulting from an increase in CO_2-content of the atmosphere. *J. Atmos. Sci.* **37,** 99–118.

Manabe, S., Bryan, K., and Spelman, M. (1979). A global ocean-atmosphere climate model with seasonal variation for future studies of climate sensitivity. *Dyn. Atmos. Oceans* **3,** 393–426.

Manabe, S., Wetherald, R. T., and Stouffer, R. J. (1981). Summer dryness due to an increase of atmospheric CO_2-concentration. *Clim. Change* **3,** 347–386.

Mitchel, J. F. B. (1979). "Preliminary Report on the Numerical Study of the Effect on Climate of Increasing Atmospheric Carbon Dioxide," Met. O. 20, Tech. Note No. II/137. Meteorological Office, Bracknell, Berkshire, U.K.

Möller, F. (1963). On the influence of changes in the CO_2 concentration in the air on the radiation balance of the earth's surface and on climate. *JGR, J. Geophys. Res.* **68,** 3877–3886.

Newell, R. E., and Dopplick, T. G. (1979). Questions concerning the possible influence of anthropogenic CO_2 on atmospheric temperature. *J. Appl. Meteorol.* **18,** 822–824.

North, G. R., Moeng, F. J., Bell, T. L., and Cahalan, R. F. (1982). The latitude dependence of the variance of zonally averaged quantities. *Mon. Weather Rev.* **110,** 319–326.

Ohring, G., and Clapp, P. (1980). The effect of changes in cloud amount on the net radiation at the top of the atmosphere. *J. Atmos. Sci.* **84**(C4), 3135–3147.

Panofsky, H. A., and Brier, G. W. (1968). "Some Application of Statistics to Meteorology." Penn. State Univ. Press, University Park, Pennsylvania.

Phillips, N. A. (1956). The general circulation of the atmosphere: A numerical experiment. *Q. J. R. Meteorol. Soc.* **82,** 132–164.

Plass, G. N. (1956). The influence of the 15 carbon dioxide band on the atmospheric infra-red cooling rate. *Q. J. R. Meteorol. Soc.* **82,** 310–324.

Ramanathan, V. (1976). Radiative transfer within the earth's troposphere and stratosphere: A simplified radiative-convective model. *J. Atmos. Sci.* **33,** 1330–1346.

Rasool, S. I., and Schneider, S. H. (1971). Atmospheric carbon dioxide and aerosols: Effects of large increases on global climate. *Science* **173,** 138–141.

Sarmiento, J. (1982). A simulation of bomb tritium entry into the Atlantic Ocean. *JGR, J. Geophys. Res.* (in press).

Schneider, S. H., and Thompson, S. L. (1981). Atmospheric CO_2 and climate: Importance of the transient response. *JGR, J. Geophys. Res.* **86**(C4), 3135–3147.

Smagorinsky, J. (1963). General circulation experiments with the primitive equations. I. The basic experiment. *Mon. Weather Rev.* **91,** 99–164.

Smagorinsky, J. (1977). Modeling and predictability. "Energy and Climate." Geophys. Res. Comm., Nat. Acad. Sci., Washington, D.C.

Taljaad, J. J., Van Loon, H., Crutcher, H. L., and Jenne, R. L. (1969). "Climate of the Upper Air. 1. Southern Hemisphere," NAVAIR 50-IC-55. U.S. Nav. Weather Ser., Washington, D.C.

Tyndall, J. (1863). On radiation through the Earth's atmosphere. *Philos. Mag.* [4] **22,** 160–194, 273–285.

Wang, W. C., Yung, Y. L., Lacis, A. A., No, T., and Hansen, J. E. (1976). Greenhouse effect due to man-made perturbation of trace gases. *Science* **194,** 685–690.

Wetherald, R. T., and Manabe, S. (1975). The effect of changing the solar constant on the climate of a general circulation model. *J. Atmos. Sci.* **32,** 2044–2059.

Wetherald, R. T., and Manabe, S. (1981). Influence of seasonal variation upon the sensitivity of a model climate. *JGR, J. Geophys. Res.* **86,** 1194–1204.

Wigley, T. M. L., and Jones, P. D. (1981). Detecting CO_2-induced climate change. *Nature* (*London*) **292,** 205–208.